©2022 Published in 6th International Symposium on Natural Hazards and Disaster Management
21-23 October 2022 (ISHAD2022 Bursa - Turkey)
https://doi.org/10.33793/acperpro.XXXX

A Preliminary Study on Long Period Ground Motion in the Eskişehir Basin, Turkey

[1]Lütfü İhsan Akpunar and [1*]Gülüm Tanırcan
[1]Kandilli Observatory and Earthquake Research Institute, Boğaziçi University, İstanbul, Turkey

Abstract

Effects of a basin structure on long period ground motion generation in Eskişehir region are studied by investigating the observed features of the 2011 Simav Earthquake (Mw:5.9) accelerograms. Spectral values and significant duration of ground motion at the basin center is much higher than the predicted mean values obtained by empirical models. 3-D wave propagation simulation of a small magnitude local event is accomplished utilizing a finite difference method and experimental velocity models. Simulation results indicate that the basin model produces more realistic waveforms than the flat layered model. Synthetic velocities agree with observed ones at two basin-center stations but considerable discrepancies exit at basin edge stations. These findings suggest that more careful definitions of basin boundaries are necessary for future models.

Key words: Numerical modeling, velocity structure, basin effects, wave propagation, Eskişehir

1. Introduction

Urbanization in valleys exposes significantly high seismic risk to earthquake-prone regions. It is now well known that the amplitude and duration of strong ground motion are governed by multiple reflection of seismic waves in the basin structures. Extensive structural damage at Mexico City during the 1985 Michoacan earthquake and in San Francisco during the 1989 Loma Prieta earthquake are just two past examples portraying how disastrous deep sedimentary basins can be on structures and human beings. Eskisehir city in Turkey, which is the case study of this study, is a specific example to these regions. The city is the home to nearly 1 million people and location for many long period structures due to rapid urbanization. The city is located at the boundary of central and western Anatolia tectonic regions. Between two active faults Eskişehir Basin extends in EW direction with two open ends. The city has been expanding towards this sedimentary basin. The earthquake of February 20, 1956 (Ms6.4) was the largest event in the vicinity in the instrumental period since 1900. Hence the objectives of this study are; to investigate the long period strong ground motion in the Eskişehir basin through the 2011 Simav Earthquake (Mw5.9) accelerograms and then long period simulation of a local event utilizing a generic 1-D horizontal velocity structure and horizontal velocity structure with basin added on top.

*Corresponding author: Address: Kandilli Observatory and Earthquake Research Institute, Boğaziçi University, İstanbul, TURKEY. E-mail address: birgore@boun.edu.tr, Phone: +902165163279

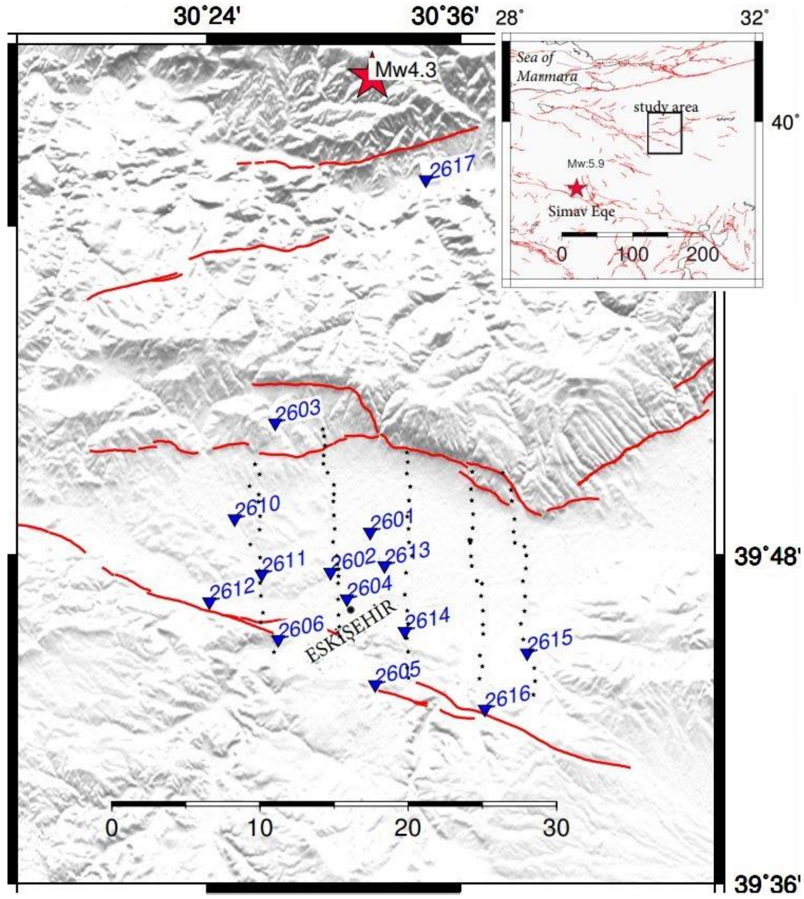

Figure 1. Location of the 2011 Simav and the 2015 Eskişehir earthquakes (red stars), strong ground motions stations (blue downward triangles), active faults surrounding Eskisehir (red lines), Microtremor array measurements (black dots).

2. Investigation of Strong Ground Motions

At Eskişehir Province, there have been twenty strong ground motion stations operated by The Disaster and Emergency Management Presidency (AFAD). Ground motion recordings are available in their respective web sites (https://tadas.afad.gov.tr/). Among them, 6 of those stations (2601, 2602, 2604, 2610, 2611 and 2613) are located at the center of the basin (Yamanaka et al., 2018).

A strong earthquake occurred on May, 2011 in Simav district of Kütahya province in Western Turkey. Moment magnitude of the earthquake is announced as Mw 5.9 by Global Centroid Moment Tensor Project (https://www.globalcmt.org). The 2011 Simav earthquake was well recorded by 14 strong motion stations located in and around Eskişehir. Epicental distances are in the range of 137-150 km.

Strong ground motions in Eskişehir are investigated in terms of amplitudes and significant duration

($T_{5\text{-}95}$). Station information, their distance measures and amplitudes are listed in Table 1. As expected, stations located outside of the basin structure such as the 2603 and 2616 have relatively simple and short waveforms. Whereas recordings of basin-edge and basin center stations such as 2610 and 2611 are characterized by their long durations. Maximum Peak Ground Acceleration (PGA) (13.3 cm/s^2) was recorded at the 2606, whereas the maximum peak ground velocity (PGV) (1.5 cm/s) was recorded by the 2610 after the arrival of S-package package.

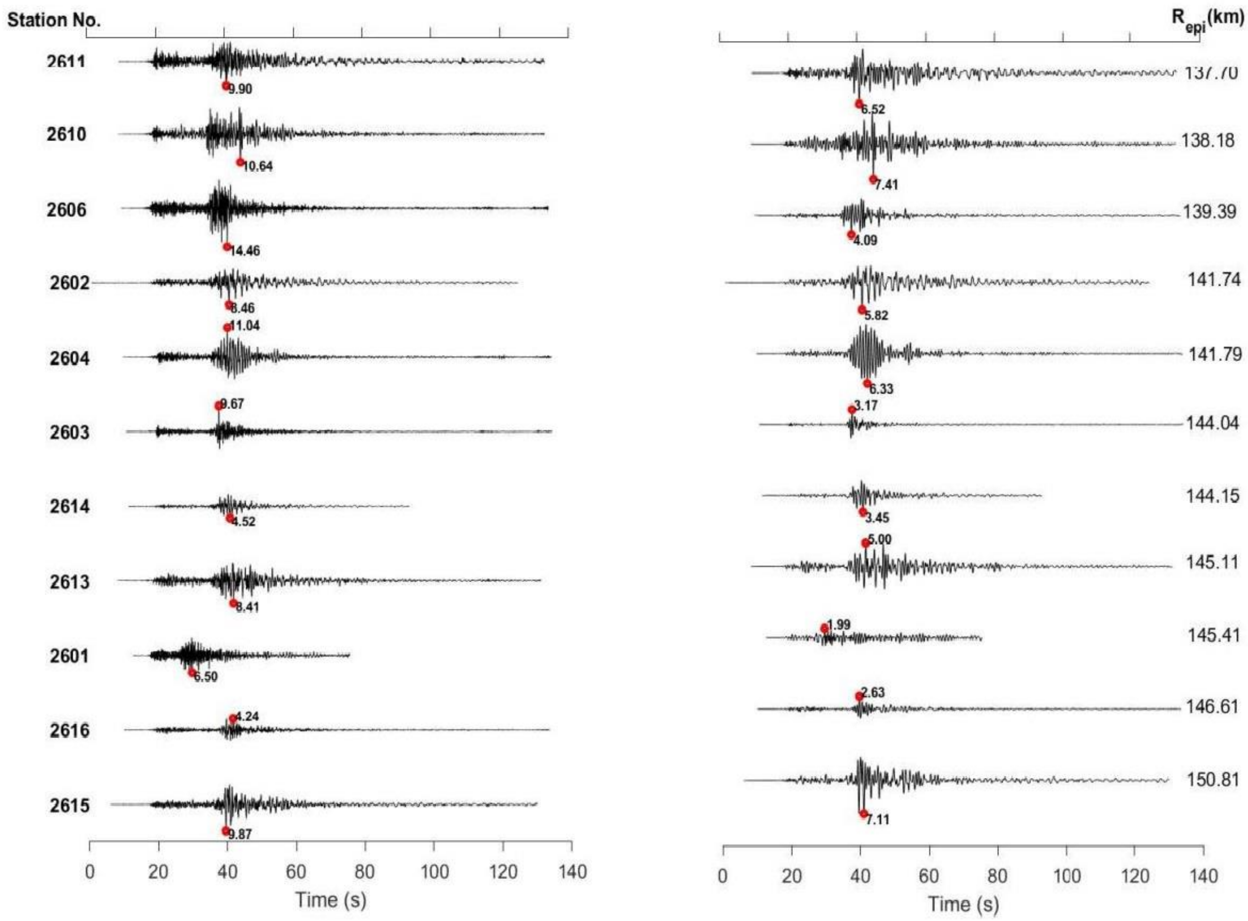

Figure 2 Raw (left) and 0.2-2 Hz band-pass filtered (right) EW component velocity recordings of the 2011 Simav earthquake (Mw 5.9)

5% damped Spectral accelerations (Sa) at 4 spectral periods (T= 0.01, 1, 2 and 3 s) are calculated and listed in Table 1. The highest values are obtained at basin-center stations. Sa at T=1 s spectral period is obtained at the 2610 whereas, the highest Sa at T=2 s and T=3 s are at the 2602 and 2611, respectively. Considerable difference in Sa at T=2 s. between the 2601 and nearby 2613 may be explained by the difference in deep velocity structures of these two location. Sa values are further compared with median values of 2 Ground Motion Prediction Equation (GMPE); Kale et al., (2015) [1] and Gülerce et al., (2016) [2] in terms of residuals (ln(Observed/Predicted)) (Figure 3). In general, values at almost all stations are higher than what is predicted by the GMPEs. The predicted mean PGA by Gülerce et al., (2016) [2] at the 2606 is half of the recorded one. Residual values at

2 s spectral period at the 2602, reach to 1.1 which indicates that calculated mean Sa is 3 times higher than predicted mean Sa.

Table 1. Station information, 5% damped spectral acceleration (Sa) and distance parameters of the Mw5.9 Simav earthquake recordings in Eskişehir. C:Basin-Center E:Basin-Edge O:Basin-Outside

No	Lon/Lat. (°)	V_{s30} (m/s)	Loc	R_{epi} (km)	R_{JB} (km)	$T_{5\text{-}95}$ (s)		PGV (cm/s)	PGA (cm/s^2)	Sa(cm/s^2)		
						N-S	E-W			T= 1s	T=2s	T=3s
2601	30.528/39.814	237	C	145.4	139.8	27.70	33.57	0.54	6.94	7.81	1.05	0.65
2602	30.497/39.789	328	C	141.7	136.1	46.16	37.06	0.92	7.04	12.56	10.07	2.98
2603	30.453/39.880	630	E	144.0	138.6	31.90	30.31	0.61	7.01	3.31	1.94	1.23
2604	30.510/39.773	296	C	141.8	136.1	36.31	24.05	0.98	9.90	16.53	4.07	1.73
2606	30.456/39.749	348	E	139.4	133.7	24.94	29.43	0.92	13.30	7.82	3.07	1.53
2607	30.146/39.817	267	O	118.9	113.7	48.36	40.81	0.88	7.30	8.96	3.42	2.98
2608	31.183/39.520	480	O	185.8	179.7	47.37	44.98	0.17	1.55	1.38	0.69	0.52
2610	30.422/39.822	407	C	138.2	132.7	30.65	32.61	1.50	11.18	18.42	5.39	2.30
2611	30.443/39.788	275	C	137.7	132.1	53.77	53.18	1.33	10.29	12.26	8.43	5.47
2613	30.540/39.794	281	C	145.1	139.5	32.42	40.94	1.14	9.89	11.60	7.11	2.13
2614	30.556/39.753	516	E	144.1	138.4	31.49	21.79	0.60	4.25	6.74	3.99	1.55
2615	30.652/39.740	307	E	150.8	145.0	40.02	31.28	1.32	7.97	16.73	7.00	3.74
2616	30.619/39.706	471	E	146.6	140.7	40.23	38.31	0.51	4.83	5.15	1.87	1.17

Although the distances of stations are almost in the same range, there is considerable difference in $T_{5\text{-}95}$ of them. It has been observed that $T_{5\text{-}95}$ has its largest value at basin-center stations. The largest significant duration is as high as 53 s, in both horizontal components at the 2611. $T_{5\text{-}95}$ gradually decreases toward basin-edge stations. For example, the geometric mean $T_{5\text{-}95}$ of the 2610, 2611 and 2606, which have the same epicentral distance, are found to be 31 s, 53 s, 26 s, respectively. Similarly, the 2602 and 2604 are located 145 km away from the epicenter and their geometric mean $T_{5\text{-}95}$ are 41 s and 29 s. Calculated $T_{5\text{-}95}$ values are further compared with predictive model suggested by Sandıkkaya and Akkar (2017) [3]. Recorded $T_{5\text{-}95}$ are within ±1 std. deviation of the empirical model. As captured from Figure 4 median values are underestimated by the prediction equation particularly for basin-center stations.

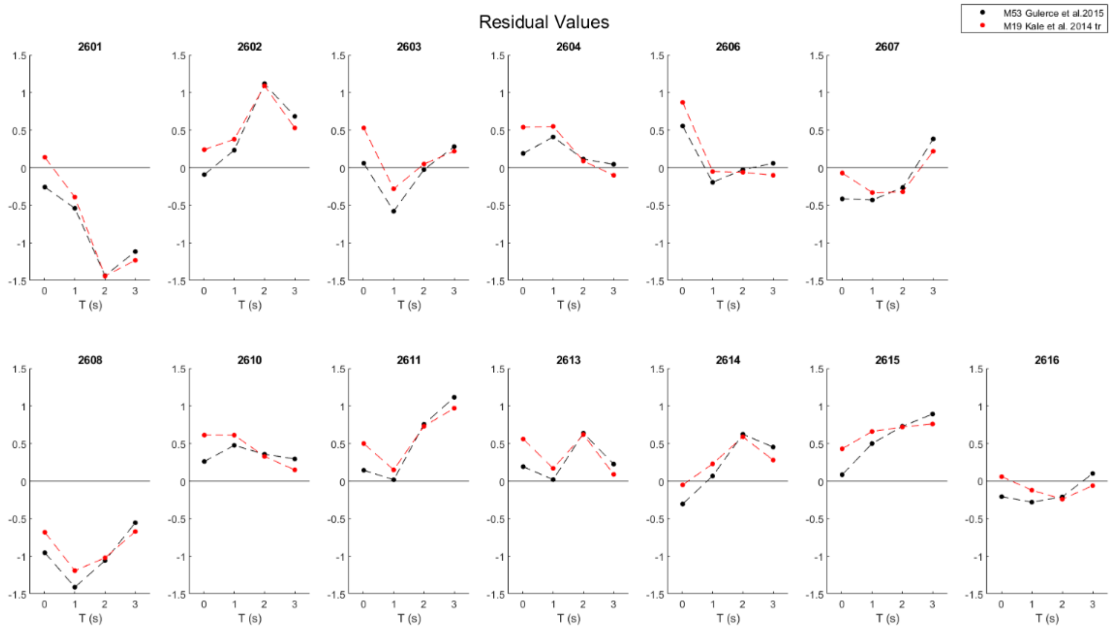

Figure 3. Residuals of spectral accelerations (Sa) at T= 0.01, 1, 2 and 3 s at 13 stations.

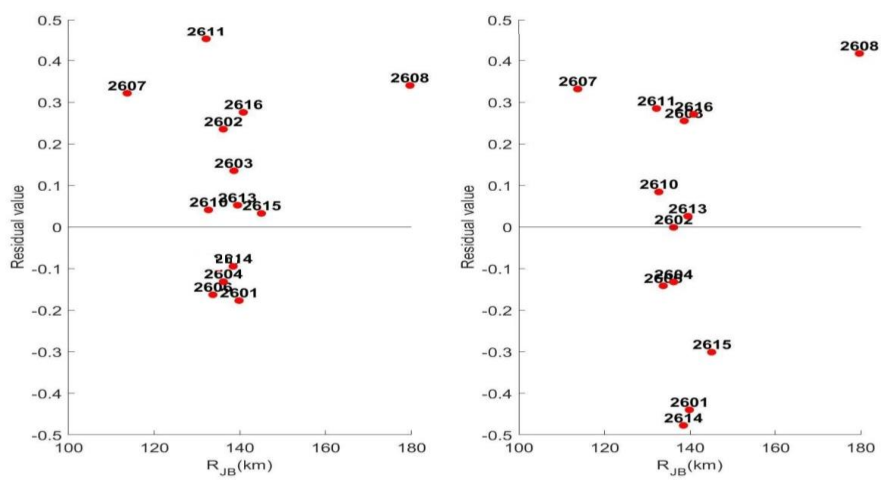

Figure 4 Residual values of $T_{5\text{-}95}$ (left), and $T_{5\text{-}75}$ (right) with respect to closest horizontal distance to rupture plane (R_{JB})

Characteristics of the later phases in basin-center stations are investigated by particle motion analyses. For instance, as in Figure 5, the 2610 and the 2611 waveforms show apparent later phase after the S wave arrival. In particle motion diagram, retrograde motions are detected. This fact indicate the later phase is a Rayleigh wave. Indeed, particle motion of box 1 in the 2610 waveform is rather complex. Hence a more complex propagation of surface waves might be considered for this motion.

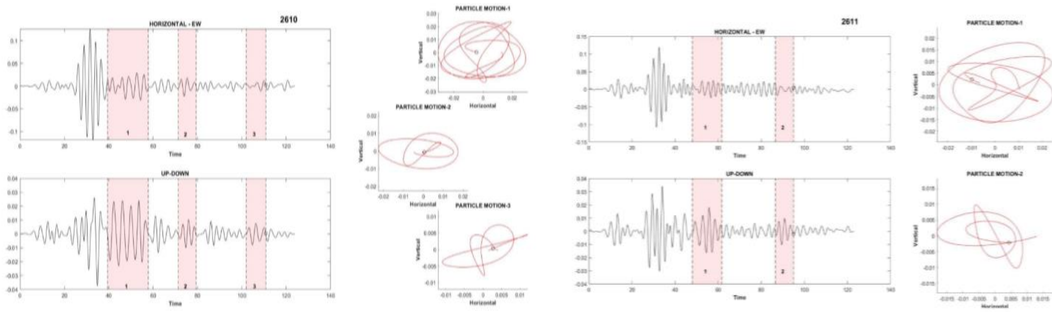

Figure 5. 0.25-0.5 Hz band-pass filtered displacement time series of the 2011 Simav Earthquake at the 2610 and 2611 stations. Particle motions of the boxes are given next to them.

3. Simulation of the Long Period Ground Motion

In this study 2 experimental velocity models are used. Flat model: horizontal velocity structure by Mindevalli and Mitchell (1989) [4] and Modified model: flat model is modified by replacing the first flat later with basin geometry, providing territorial variations remain constant (Figure 6). Site-specific investigations conducted by Özel et al. (2020) [5]; Tün et al. (2016) [6]; Yamanaka et al. (2018) [7] were utilized to construct the basin geometry. The seismic velocity is the same for each model. Microtremor array measurement (MAMs) points are obtained from Tün et al. (2016) and TUBITAK-116Y524 project report (Özel et al., 2020) [5]. The bedrock depth is determined utilizing the relationships between the resonance frequency and bedrock depth proposed by Tün et al. (2016). The maximum depth of the bedrock was found at almost 650 m in the northeastern part (Figure 7). Dimensions of the model are 43 km x 27 km x 15 km. In the modified model, basin layer continues across the entire model in EW direction, but bordered by northern and southern hills to mimic the geographical environment. Top layer has the following properties; Vp:2.70 km/s Vs:1.3 km/s density= 2.1 g/cm^3 Q=200, grid spacing is 100 m in for the first 3 km in depth direction, while grid increment is 200 m in horizontal directions. The max frequency the simulation can successfully produce is 2.1 Hz.

3D wave propagation of a small magnitude event (Mw4.3) occurred at north of the region (Table 3) is performed and synthetics are compared with observed recordings (Figure 8). The computer code utilizes a finite difference modelling using staggered grids with non-uniform spacing (Pitarka, 1999) [8].

The results with flat model show that, amplitude of synthetics in the NS direction is far more than those of observed waveforms, where in the EW direction, simulated waves generally agree with the observed waveforms in frequency range of 0.3-1 Hz, except the 2615. Modified model improves harmonization of observed and synthetic amplitudes at two basin stations the 2610 and the 2612, in the NS direction. The phase compatibility shows good agreement in the E-W direction for the flat model when compared modified model. On the contrary, the modified model increases the compatibility in phase and amplitude for the N-S direction.

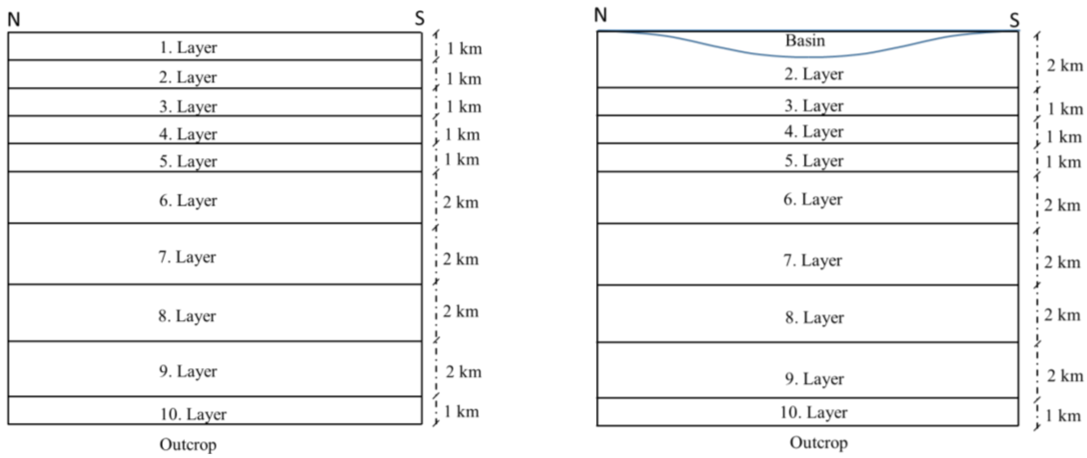

(a) (b)

Figure 6. Velocity Structure Model for Eskişehir used in the simulation. (a) Flat Model: Model by Mindevalli and Mitchell (1989), (b) Modified Model: Model by Mindevalli and Mitchell added basin structure on top

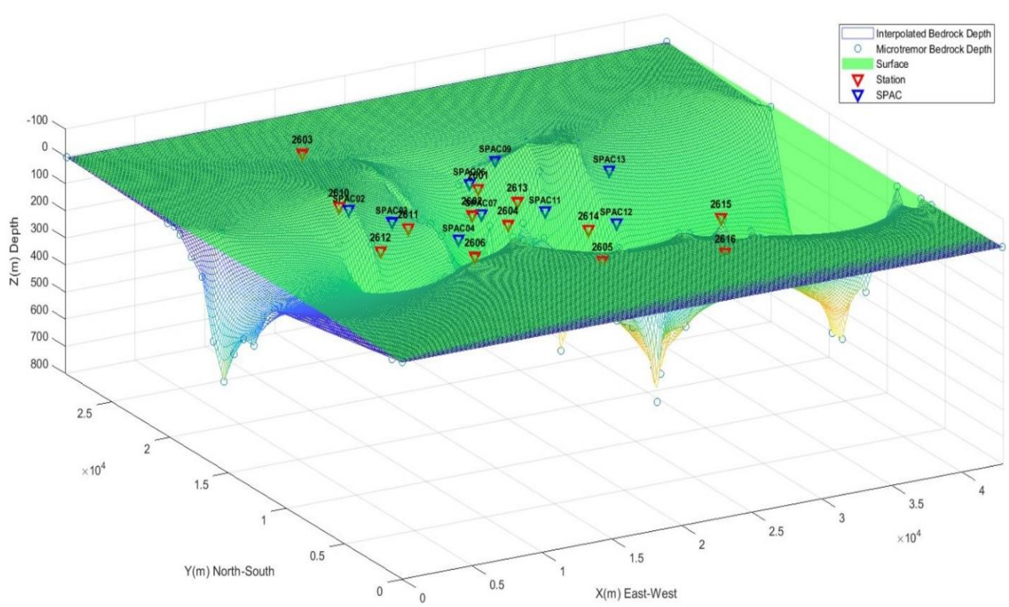

Figure 7. The 3D appearance of the basin from West to East.

Table 3. Moment tensor solution of Eskişehir Earthquake Mw 4.3 from the (ISC, http://www.isc.ac.uk)

Date-Time (UTC)	Location		Mw	Depth (km)	Mo (dyne*cm)	Strike * (°)	Dip (°)	Rake (°)
	Latitude	longitude						
17.01.2015	40.09°	30.53°	4.3	10	3.04E+22	273	82	-86

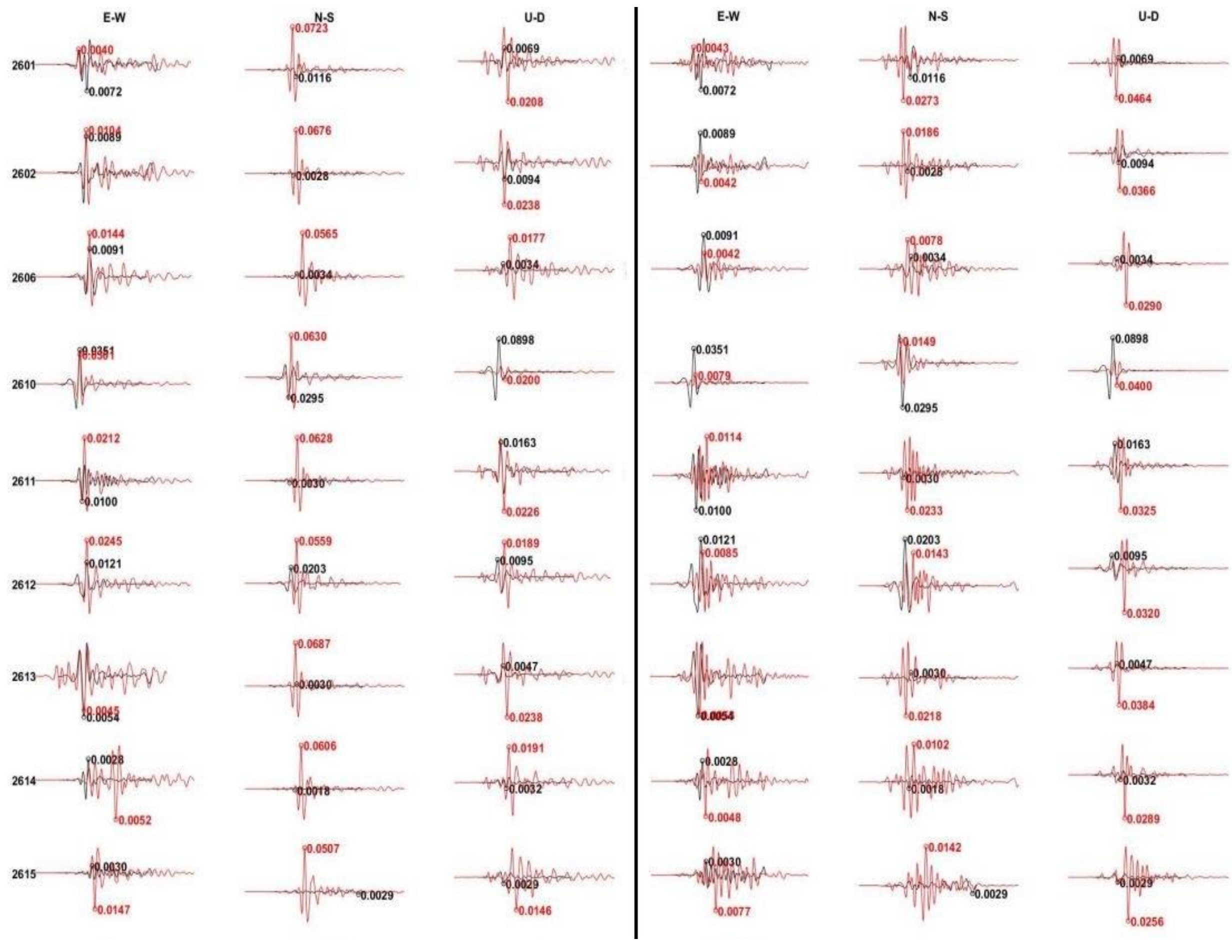

Figure 8. Comparison between observed (in black) and synthetic (in red) velocity time series (cm/s) of the Mw 4.3 earthquake. Waveforms are band-pass filtered at 0.3-1 Hz. Left side obtained by using the flat velocity model, right side acquired from modified velocity.

4. Conclusions

In this study, the 2011 Simav earthquake is examined to characterize the features of the motion at Eskişehir basin during the earthquake in terms of the duration, 5 % damped elastic spectral ordinates at different period. Long-period ground motion modeling in Eskişehir basin is also studied with a 3-D substructure model, which was constructed using a horizontally layered velocity structure and a horizontally layered velocity structure with a basin geometry added on top.

The numerical simulation with the flat model shows good matching with the 2015 Mw 4.3 earthquake in EW direction in the frequency range between 0.3 and 1 Hz. The modified model has improved the waveforms in NS. However, there were challenges in producing time series to be in agreement with recorded seismograms in the NS direction. Outcomes indicate that the velocity structure is more complex than the model utilized in the simulation. Moreover, the spatial variability might be beyond the predicted value. The discrepancy between synthetics and real data may stem from the velocity contrast and representation of the basin with a single layer. Further

field investigations is necessary to improve the velocity structure model.
This study is the first step towards the long period simulation of the ground motion at this region. Here it is not intended to refine the basin model, instead, to test the adequacy of the initial basin model calculated with the available data.

Acknowledgements

This study was supported by Boğaziçi University Research Fund Grant Number 19201. We would also like to thank to Eşref Yalçınkaya for sharing site predominant frequency information obtained in Eskişehir.

References

[1] Gülerce, Z., B. Kargoığlu and N. A. Abrahamson. Turkey-adjusted NGA-W1 horizontal ground motion prediction models. Earthquake Spectra 2016;32;75-100.

[2] Kale, Ö., S. Akkar, A. Ansari and H. Hamzehloo. A ground-motion predictive model for Iran and Turkey for horizontal PGA, PGV, and 5% damped response spectrum: Investigation of possible regional effects. Bulletin of the Seismological Society of America 2015;105;963-980.

[3] Sandıkkaya, M. A. and S. Akkar. Cumulative absolute velocity, Arias intensity and significant duration predictive models from a pan-European strong-motion dataset. Bulletin of Earthquake Engineering 2017;15;1881-1898.

[4] Mindevalli, O. Y. and B. J. Mitchell. Crustal structure and possible anisotropy in Turkey from seismic surface wave dispersion. Geophysical Journal International 1972; 98;93-106.

[5] Özel, O., E. Yalcinkaya, G. Birgoren, M. Tün, E. Pekkan, O. Kaplan. Kabuk depremleri nedeniyle oluşan Kuvvetli yer hareketinin tahmini için jeolojik yapıların modellemesi ortak araştırması. 2020; TUBITAK 1001 Project, Projct Code: 116Y524.

[6] Tün, M., E. Pekkan, O. Özel and Y. Guney. An investigation into the bedrock depth in the Eskisehir Quaternary Basin (Turkey) using the microtremor method. Geophysical Journal International 2016;207;589-607.

[7] Yamanaka, H., Ö. T. Özmen, K. Chimoto, M. A. Alkan, M. Tün, E. Pekkan, O. Özel, D. Polat and M. Nurlu. Exploration of S-wave velocity profiles at strong motion stations in Eskisehir, Turkey, using microtremor phase velocity and S-wave amplification", Journal of Seismology. 2018;22;1127-1137.

[8] Pitarka, A. 3D elastic finite-difference modeling of seismic motion using staggered grids with nonuniform spacing", Bulletin of the Seismological Society of America. 1999;89;54-68